Mathematical Biosciences and Engineering

http://www.aimspress.com/journal/mbe

MBE, 22(5): 1185–1205.
DOI: 10.3934/mbe.2025043
Received: 13 December 2024
Revised: 19 March 2025
Accepted: 01 April 2025
Published: 10 April 2025

Research article

Modelling human response to information in voluntary vaccination behaviour using epidemic data

Bruno Buonomo[1,*] **Rossella Della Marca**[1] **and Manalebish Debalike Asfaw**[2]

[1] Department of Mathematics and Applications, University of Naples Federico II, via Cintia, Naples, I-80126, Italy

[2] Department of Mathematics, University of Addis Ababa, Addis Ababa, Ethiopia

* **Correspondence:** Email: buonomo@unina.it.

Abstract: Here, we considered Holling functional responses, a core concept in population dynamics, and discussed their potential interpretation in the context of social epidemiology. Then, we assessed which Holling functional response best represents the vaccination behaviour of individuals when such a behaviour is influenced by information and rumours about the disease. In particular, we used the Holling functionals to represent the information-dependent vaccination rate in a socio-epidemiological model for meningococcal meningitis. As a field case test, we estimated the information-related parameters by using official data from a meningitis outbreak in Nigeria and numerically assessed the impact of the functionals on the solutions of the model. We observed significant inaccuracies on parameter estimates when either Holling type I or Holling type III functional were used. On the contrary, when the Holling type II functional was employed, epidemiological data were well reproduced, and reasonable values of the information parameters were obtained. Given the socio-epidemiological interpretation of the Holling type II functional, this means that the rate at which susceptible individuals come into contact with information may be assumed to be constant and that the time needed to handle the available information cannot be neglected.

Keywords: mathematical epidemiology; vaccination; information; human response; meningitis; Holling functionals

1. Introduction

When dealing with infectious diseases, the individual choices regarding the adoption of protective measures such as vaccination, quarantine, or social distancing are determining factors for the success of mitigation strategies, especially when information and rumours on the disease status cause significant social alarm [1]. For this reason, the impact of human behavioural changes on the epidemic

dynamics of infectious diseases is increasingly attracting the attention of scholars working in many fields, including mathematics [2].

The behavioural epidemiology of infectious diseases (BEID) is a recent but already well-established field that focuses on mathematical modelling in epidemiology where the feedback between human behaviour and disease spread is considered [3–5]. Epidemic models including the effects of human behavioural changes may be dated back to 1970s, when V. Capasso hypothesised that the force of infection, i.e., the number of infections per unit time, must be in some cases represented by a nonlinear function of the prevalence of the disease. Indeed, the growth of the force of infection may slow down as the prevalence increases as a consequence of human response to the increased risk of contagion [6, 7].

A key factor influencing individual choices is the awareness regarding both the disease and the protective measures against the risk of infection [8]. The public awareness, in turn, is influenced by information (and rumours) circulating within the population and takes time to build since the process of information transfer consists in articulated routine procedures [9]. In addition, individuals will also act according to their previous experience with disease trends. Therefore, delay and memory are two fundamental aspects of the opinion-driven change in behaviour. From the BEID modelling perspective, these two aspects can be taken into account through the introduction of the so-called *information index*. This index is a measure of the individuals' awareness and depends on both current and past circulating information about the disease spread [4, 5]. The BEID models that include the information index (say, *behavioural models*) extend the early idea of Capasso [10].

In a series of papers starting in 2007, P. Manfredi, A. d'Onofrio, and coworkers studied relatively simple SIR (Susceptible-Infectious-Recovered) and SEIR (Susceptible-Exposed-Infectious-Recovered) models augmented with the information index [11–13]. These studies were mainly theoretical and showed that self-sustained oscillations may occur depending on the information-related functions. Therefore, it can be concluded that recurrent epidemic waves may be induced by individuals' behavioural changes.

Later on, the information index was embedded in models with more complex structures (see, e.g., [14, 15]). However, only in more recent times have information index-augmented models been applied to real-world epidemics using official data provided by public health systems [16, 17].

Human responses to information strictly depend on the specific case considered. For example, people may be very willing to adopt social distancing if there are no other protective measures, but they may dislike and/or disregard it if there is a high level of protection in the population, such as high vaccination coverage [18, 19]. As a consequence, a key aspect of behavioural models is the link between epidemic evolution and human awareness, which is the formulation of the functions describing the population's response to the information.

A common assumption in BEID is that the adoption rate of a given protective measure (e.g., vaccination rate, quarantine rate) saturates; in other words, it increases until it reaches a constant maximum value as the information index increases. Such a relationship between adoption rates and the information index is typically described by Holling functional responses [11, 13, 20]. As is well known, the Holling functional responses were introduced in ecological modelling by C.S. Holling in 1959 [21, 22] and are still widely used in that field [23]. Holling functionals are generally classified into three types. Type I is a continuous linear function that increases up to a maximum threshold which it is constant; type II is a function that saturates while preserving concavity; and type III is a sigmoid saturating function. Therefore, in the context of BEID, Holling functional responses describe different possible

behaviours of the population. For example, compared with type II, type III represents a population with a lower (resp. higher) response when the level of social alarm is low (resp. high).

To our knowledge, there are no studies in the literature that focus on how to select the functional responses that best represent the behaviour of the population under consideration. Therefore, in this paper, we propose a contribution in this direction by testing the ability of an epidemic model, where the population's response to information is represented by different Holling functionals, to reproduce real data.

In a recent paper, we proposed a socio-epidemiological model with information index to investigate the vaccine hesitancy in meningococcal meningitis transmission [17]. The model is given by a system of six nonlinear ordinary differential equations and is based on a previous SCIR model (Susceptible–Carrier–Ill–Recovered). The information index is included in the model to take into account that the willingness of individuals to get vaccinated depends on the information and rumours about the disease status within the community. The model in [17] was used to reproduce both the uncontrolled phase and the vaccination campaign of the meningitis epidemic that occurred in Nigeria in 2016. The model allowed to estimate the values of relevant information parameters, such as the information coverage and the characteristic memory length. A Holling type II functional was used to represent the information-dependent vaccination rate. However, the lack of field data on vaccinating attitudes makes it necessary to explore the potentially better performance of other functional responses in reproducing the reactivity of individuals.

Motivated by the above considerations, we reconsider the socio–epidemiological model introduced in [17]. We first assume that the vaccination rate is a generic information-dependent function and perform a qualitative analysis based on stability and bifurcation theory. Then, by following pioneering works on the use of Holling functions in predator-prey dynamics, we provide an interpretation of these functions in the context of socio-epidemiology. We numerically investigate the solutions of the model when different Holling functional responses are employed as information-dependent vaccination rate. The solutions are compared with official data on the meningitis epidemic in Nigeria. The values of the information coverage, the characteristic memory length, and the reactivity factor to voluntary vaccination are estimated for each of the considered cases. Finally, two indexes, the relative change of the total cases of illness (RCCI) and the relative change of the total deaths (RCCD) are used to assess which type of functional is most appropriate to represent the individual behavioural response.

The remainder of the manuscript is organised as follows. In Section 2, we present the meningitis model with information-dependent vaccination, named SCVIR–M, and investigate some of its basic properties. In Section 3, we provide a socio-epidemiological interpretation of the Holling functions. Section 4 is devoted to the parametrisation of the model, based on the official data from the outbreak of meningitis in Nigeria. In Section 5, we compare the impact of the use of each Holling function on the solutions of the SCVIR–M model. Concluding remarks are given in Section 6. The manuscript is finally complemented by an Appendix containing some details on the qualitative analysis of the model.

2. The model

In this section, we recall the socio-epidemiological meningitis model proposed in our previous study [17]. A population is considered where, at time t, individuals are divided into five disjoint compartments, the sizes of which are the state variables of the model: susceptible individuals, $S(t)$;

vaccinated, $V(t)$; carriers, $C(t)$; ill individuals, $I(t)$; and recovered, $R(t)$. The size of the total population is denoted by N (therefore, $N = S+V+C+I+R$). It is assumed that vaccinated individuals receive partial and temporary protection by immunisation, and that vaccination is partially determined on a voluntary basis. Therefore, the individual decisions to vaccinate oneself partially depend on the information and rumours on the status of the disease in the community. In other words, the vaccination rate is assumed to depend on the information index M [4, 5]. The balance equations for each compartment are given by the following system of nonlinear ordinary differential equations, which is a *behavioural* extension of previously studied meningitis models [24, 25]:

$$\begin{aligned}
\dot{S} &= \Lambda - \beta S \frac{C+I}{N} - p(M)S + \theta V + \phi R - \mu S \\
\dot{V} &= p(M)S - (1-\psi)\beta V \frac{C+I}{N} - (\theta+\mu)V \\
\dot{C} &= \beta\left(S + (1-\psi)V\right)\frac{C+I}{N} - (\sigma+\delta+\mu)C \\
\dot{I} &= \sigma C - (\rho+\mu+\nu)I \\
\dot{R} &= \delta C + \rho I - (\phi+\mu)R,
\end{aligned} \tag{2.1}$$

where the upper dot denotes the time derivative. All parameters are positive constants: Λ is the net inflow of susceptibles; β is the disease transmission rate; θ and ϕ are the waning rates of vaccine-induced and disease-induced immunity, respectively; μ is the natural mortality rate; $\psi \leq 1$ is the factor of vaccine effectiveness in reducing the disease transmission ($\psi = 1$ means that the vaccine fully prevents from infection); σ is the rate at which carriers develop symptoms; δ and ρ are the recovery rates for carriers and ill individuals, respectively; and ν is the disease-induced mortality rate.

In model (2.1), the information-dependent vaccination rate is formulated as follows:

$$p(M) = p_0 + p_1(M). \tag{2.2}$$

This formulation takes into account two important aspects of vaccine acceptance. First, part of the population gets vaccinated independently from the information regarding the status of the disease, since they are pro-vaccine or strictly follow the recommendations of public health planners [26, 27]. The information-independent vaccination is the positive parameter p_0 in (2.2). Second, part of the population chooses to get vaccinated due to the social alarm caused by the disease. Hence, the function $p_1(M)$ in (2.2) describes the response of the population to information. It is required to be a continuous, differentiable (except at a finite number of points), and increasing function such that

$$p_1(0) = 0; \quad p_0 + \sup(p_1) = p_{\max} < +\infty. \tag{2.3}$$

Now, it remains to be described the information index M in our specific case. The choice of individuals to get vaccinated or not is assumed to depend on the present and past* information they collect on the spread of the disease, where past information is weighted in an exponential way. It is assumed that people react in response to information and rumours regarding the ill cases in their community. More precisely, the perceived risks associated to meningitis are assumed to be proportional to the size of the compartment I.

*Here, we intend as *past* the period from a given initial time, say $t = 0$, to the current time.

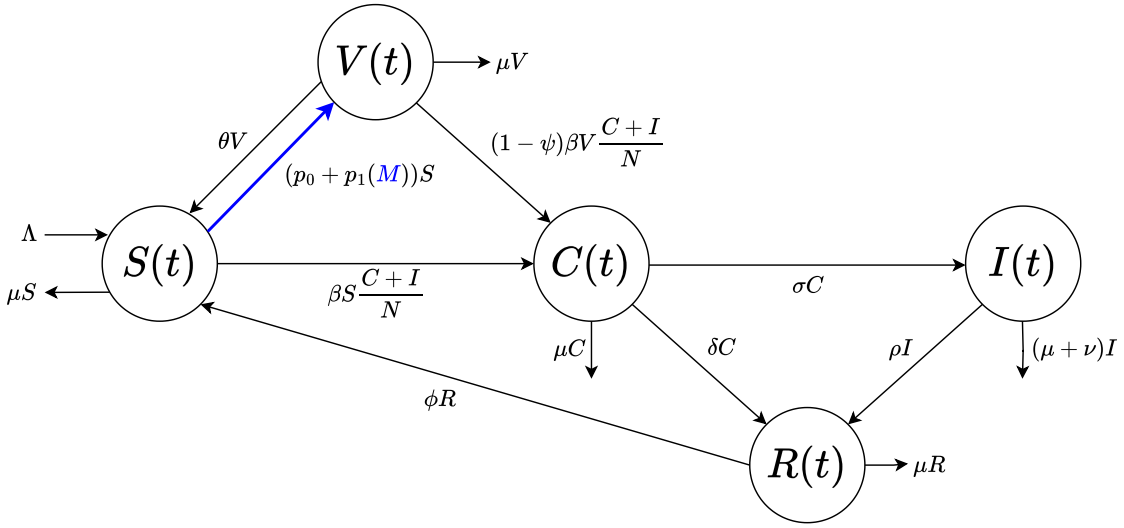

Figure 1. Flowchart of the meningococcal meningitis SCVIR–M model. The total population $N(t)$ is divided into five disjoint compartments: susceptible $S(t)$, vaccinated $V(t)$, carriers $C(t)$, ill $I(t)$, and recovered individuals $R(t)$. Blue colour indicates the information-dependent process, where $M(t)$ is the information index (2.4).

Summarizing, the information index is given as follows:

$$M(t) = \int_{-\infty}^{t} k\frac{I(\tau)}{\bar{N}} H(\tau) a e^{-a(t-\tau)} d\tau, \tag{2.4}$$

where the parameter k is the *information coverage*, which is set $k \in (0, 1]$ to represent the phenomenon of under-reporting [11], and $\bar{N} = \Lambda/\mu$ is a reference value[†]. H denotes the Heaviside step function, which is introduced to limit the time interval of the relevant information from $(-\infty, t)$ to $(0, t)$, where $t = 0$ represents the initial time. The exponentially fading memory kernel, $a \exp(-a(t-\tau))$, describes an exponential decay of the memory of individuals, with characteristic memory length $1/a$, which can be interpreted as the average time delay in the collection of the information on the disease [5].

From (2.4), by applying the linear chain trick [28], we obtain the differential equation ruling the dynamics of M:

$$\dot{M} = a(hI - M), \tag{2.5}$$

where $h = k/\bar{N}$.

We refer to equations (2.1)–(2.2)–(2.5) as SCVIR–M model. The state variables and the processes included in the model are illustrated in the flowchart in Figure 1. A description of each model parameter together with its baseline value is given in Table 1 in Section 4.

The initial conditions associated with the SCVIR–M model are:

$$\begin{aligned} &S(0) = S_0 > 0,\ V(0) = V_0 \geq 0,\ C(0) = C_0 \geq 0, \\ &I(0) = I_0 \geq 0,\ R(0) = R_0 \geq 0,\ M(0) = M_0 \geq 0. \end{aligned} \tag{2.6}$$

[†] $\bar{N}$ is the steady state of the total population in absence of the disease or when $\nu = 0$, see Appendix A.

The solutions of the model are epidemiologically well-posed since the region

$$\Omega = \left\{ (S, V, C, I, R, M) \in \mathrm{R}^6_+ \;\middle|\; S > 0,\ S + V + C + I + R \leq \frac{\Lambda}{\mu},\ M \leq k \right\}, \tag{2.7}$$

is positively invariant. This is proved in [17], where it is also shown that the basic reproduction number of the SCVIR–M model is given by

$$\mathcal{R}_0 = \beta \frac{\rho + \mu + \nu + \sigma}{(\sigma + \delta + \mu)(\rho + \mu + \nu)}, \tag{2.8}$$

and the control reproduction number is given by

$$\mathcal{R}_V = \mathcal{R}_0 \frac{(1 - \psi)p_0 + \theta + \mu}{p_0 + \theta + \mu}. \tag{2.9}$$

In Appendix A, a qualitative analysis based on existence and stability of equilibria is reported, including a bifurcation analysis, that reveals that $\mathcal{R}_V = 1$ is a threshold value, above which the disease may persist in the population.

3. Modelling human response to information

An important modelling issue that arises when assessing the impact of information on vaccination behaviour is how to choose the information-dependent part of the vaccination rate, i.e., the function $p_1(M)$ in (2.2). As already mentioned, a common requirement is that such a rate grows until a constant maximum value as the information index increases. At this aim, the function $p_1(M)$ is usually described by the Holling type II function, see e.g., [13, 14, 20]. However, both Holling type I and type III also satisfy the saturation requirement and could be, in principle, adopted.

Since the Holling functions have been introduced in the context of predator–prey dynamics, here we reinterpret such functionals in the framework of socio-epidemiology. Preliminarily, let us consider a given time interval $\mathcal{I}$ of length T_t and rethink $p_1(M)$ as the rate at which susceptible individuals come into contact with information during such time interval. In other words, $p_1(M)$ may be thought as the ratio between the amount of information available during the time interval $\mathcal{I}$ and the length of the time interval T_t. By following the Holling approach [21, 22], we assume that $T_t = T_s + T_h$, where T_s is the length of the time interval during which individuals are exposed to information and may collect it, and T_h is the *handling time* of the information (the time needed to gain awareness and react). Then, $p_1(M)$ can be modelled through the following functions:

H1. According to Holling type I formulation, $p_1(M)$ is a linear function of the information index M, which becomes constant for M exceeding a given threshold $\tilde{M}$. Specifically, taking account of (2.3), if $M > \tilde{M}$, then $p_1(M) = p_{\max} - p_0$. Otherwise,

$$p_1(M) = \frac{\alpha T_s M}{T_t}, \tag{3.1}$$

where $\alpha T_s M$ is the amount of information available during the interval $\mathcal{I}$. The parameter α is a constant of proportionality that, following Holling's terminology [22], can be named *discovery*

rate of the information. In some sense, α is a measure of the *speed* at which susceptible individuals come into contact with the information. The type I response is based on the assumption that the information is instantaneously handled, $T_h = 0$, and therefore $T_t = T_s$. In short, $p_1(M)$ can be written in compact form as

$$p_1(M) = (p_{\max} - p_0) \min\left\{\frac{DM}{(p_{\max} - p_0)T_s}, 1\right\}, \tag{3.2}$$

where $D = \alpha T_s$. From (3.2), it follows that $\tilde{M} = (p_{\max} - p_0)T_s/D$.

H2. The Holling type II functional response is based on the assumption that susceptible individuals need time, say T_h, to handle the available information. The time T_h can be expressed as

$$T_h = t_h \alpha T_s M,$$

that is the product between the amount of information available during the interval $\mathcal{I}$, i.e., $\alpha T_s M$, and the inverse of the handling speed of the information, say t_h. This yields

$$p_1(M) = \frac{\alpha T_s M}{T_s + t_h \alpha T_s M} = \frac{DM}{t_h(T_s/t_h + DM)}, \tag{3.3}$$

where $D = \alpha T_s$.

H3. The Holling type III formulation requires $p_1(M)$ to be a sigmoid function of the information index M:

$$p_1(M) = \frac{DM^2}{t_h(T_s/t_h + DM^2)}. \tag{3.4}$$

It can be obtained from the Holling type II response by supposing that the discovery rate of the information is linearly increasing with M, i.e., by replacing α with αM in (3.3). The idea behind this assumption is that in epochs of high level of prevalence I (and, in turn, of M; see (2.4)), the individuals are more likely to collect information, which leads to an information-dependent discovery rate.

4. Parametrisation using epidemic data

The parametrisation of the model is based on official data from the largest-ever global epidemic of serogroup C meningitis in Nigeria that occurred in November 2016 [29]. At that time, an unknown febrile illness began affecting individuals in the state of Zamfara, initially mistaken for severe malaria. However, in early 2017, laboratory results confirmed the disease as meningococcal meningitis caused by serogroup C. The outbreak quickly spread across Nigerian states, escalating into a widespread epidemic with a peak in cases and deaths around epidemiological weeks 14 and 15 of 2017. Vaccination campaigns started in April 2017, targeting high-risk individuals aged 1 to 29 in the most affected areas. By May 2017, approximately 2.1 million people were vaccinated. The outbreak was officially declared over by June 23, 2017. Vaccination efforts were supported by social mobilisation activities, including community outreach and media engagement, to increase awareness and promote vaccine acceptance, ultimately helping to control the spread of the disease [30, 31].

The Nigerian outbreak provides a suitable framework for testing behavioural models. In fact, meningitis is a disease that, due to the severity of its consequences, triggers a very strong behavioural

Table 1. Temporal horizon, initial conditions, and parameters values for the SCVIR–M model. The baseline values are taken from [17], except for D, k, and a that are estimated in Section 4 and reported in Table 2.

Parameter	Description	Baseline value
t_f	Temporal horizon	27 weeks
$\bar{N}$	Total population in absence of the disease	186,121,000
V_0	Initial number of vaccinated individuals	0
C_0	Initial number of carriers	$10I_0$
I_0	Initial number of ill individuals	14
R_0	Initial number of recovered individuals	0
M_0	Initial value of the information index	hI_0
Λ	Net inflow of susceptibles	$\mu\bar{N}$
$\mathcal{R}_0$	Basic reproduction number	1.889
μ	Natural mortality rate	$1/54$ years^{-1}
β	Transmission rate	0.27 days^{-1}
p_0	Information-independent vaccination rate	$0 - 0.01p_{\max}$
$p_{\max}$	Upper bound of vaccination rate	0.01 days^{-1}
ψ	Factor of vaccine effectiveness	0.85
θ	Waning rate of vaccine-induced immunity	1/5 years^{-1}
σ	Rate at which carriers develop symptoms	0.0051 years^{-1}
δ	Recovery rate for carriers	1/7 days^{-1}
ρ	Recovery rate for ill individuals	0.1128 days^{-1}
ν	Disease-induced mortality rate	0.01 days^{-1}
ϕ	Waning rate of natural immunity	0.0032 days^{-1}
D	Reactivity factor to voluntary vaccination	See Table 2
k	Information coverage	See Table 2
a	Inverse of information delay	See Table 2

response [30, 31]. Additionally, data from the Nigeria Centre for Disease Control were provided in great detail [29]. These data were used in a previous study to estimate the model parameters when $p_1(M)$ is represented by a Holling type II function [17]. We take all the baseline values from there (see Table 1), except for the information–related parameters D, k, and a, whose estimates are discussed in this section.

We observe that the quantities introduced in Section 3, namely T_s and t_h (as well as T_h, which can be derived from these ones), are strictly related to the information-seeking behaviour of individuals [32]. To the best of our knowledge, surveys on information–seeking behaviours from which we can directly infer the values of T_s and t_h are not yet available in the literature. Therefore, we use an alternative approach. First, we set $t_h = (p_{\max} - p_0)^{-1}$ in (3.3) and (3.4) to impose the required condition $\sup(p_1) = p_{\max} - p_0$. Then, we do the same for T_s and set $T_s = (p_{\max} - p_0)^{-1}$ in (3.2), (3.3), and (3.4). This leads to the Holling functions reported below.

$$\text{H1:} \qquad p_1(M) = (p_{\max} - p_0)\min(DM, 1)\,; \tag{4.1}$$

$$\text{H2:} \qquad p_1(M) = (p_{\max} - p_0)\frac{DM}{1+DM}; \tag{4.2}$$

$$\text{H3:} \qquad p_1(M) = (p_{\max} - p_0)\frac{DM^2}{1+DM^2}. \tag{4.3}$$

The reactivity factor to voluntary vaccination, D, has been estimated in case H2 assuming that the cumulative number of vaccinated individuals grows linearly in the initial phase of the vaccination campaign [17]. In order to estimate the value of D in cases H1 and H3, we use the formulation (4.1)–(4.3), which results in a nonlinear algebraic system of equations once a reference value for the information index M, say $M = M^*$, is fixed. That said, let us denote by D_{H1}, D_{H2}, D_{H3} the values of the reactivity factor D in cases H1, H2, H3, respectively. Then, by equalising the expressions (4.1)–(4.2)–(4.3) at $M = M^*$, one obtains

$$D_{\text{H1}} = \frac{D_{\text{H2}}}{1 + D_{\text{H2}}M^*}, \quad D_{\text{H3}} = \frac{D_{\text{H2}}}{M^*}. \tag{4.4}$$

Some studies highlight that high vaccination coverage for meningitis is achieved despite people doubting the effectiveness of the vaccine [33]. As a result, it appears reasonable to assume that epochs of heightened social alarm lead to high adherence to voluntary vaccination. From the modelling perspective, this circumstance should be realised independently of the mathematical form chosen to represent the human response. Therefore, as first reference value for M, we consider the case in which no mitigation actions have been implemented and select $M^* = \hat{M}_{\text{nv}}$, where $\hat{M}_{\text{nv}}$ is given by

$$\hat{M}_{\text{nv}} = \max_{[0,t_f]} \frac{\hat{I}(t)}{\bar{N}} = \frac{\hat{I}}{\bar{N}} \approx 1.4 \cdot 10^{-5},$$

with $\hat{I}(t)$ being the prevalence of the SCVIR–M model with $p_0 + p_1(M) = 0$. Note that, given the value of $\bar{N}$ in Table 1, the peak of prevalence predicted by the model in the absence of mitigation actions is $\hat{I} = 2,579$.

Furthermore, we consider also another case of different order of magnitude. Precisely, we select $M^* = \hat{M}_{\text{H2}}$, where $\hat{M}_{\text{H2}}$ is half of the maximum value reached by the information index $M(t)$, as predicted by the SCVIR–M model with (4.2). Using the results provided in [17], we get

$$\hat{M}_{\text{H2}} = \max_{[0,t_f]} \frac{M(t)}{2} \approx 4.7 \cdot 10^{-6}.$$

Once obtained the value of D, we estimate the information coverage, k, and the inverse of the information delay, a. Following [17], we search for the pair (k, a), which gives:

$$(k_{\min}, a_{\min}) = \arg\min_{(k,a)} |\text{CV}_o - \text{CV}_m|, \tag{4.5}$$

where CV_o is the official number of total vaccinated individuals during the vaccination campaign (namely, $\text{CV}_o = 2.1 \cdot 10^6$ individuals), and CV_m is the same quantity as predicted by the SCVIR–M model, that is

$$\text{CV}_m = \int_0^{t_f} (p_0 + p_1(M(t)))\, S(t) dt.$$

Numerical simulations are performed using the `ode45` solver in Matlab [34]. The estimated values

Table 2. Parameter values and index estimates through the SCVIR–M model. First column: reference value of the information index, M^*. Second column: type of Holling functional response. Third, fourth, and fifth columns: estimated values of the reactivity factor, D, information coverage, k, and inverse of information delay, a, respectively. Sixth column: relative change of the total cases of illness w.r.t. the unresponsive case, RCCI. Seventh column: relative change of the total deaths w.r.t. the unresponsive case, RCCD. Initial conditions and remaining parameter values are given in Table 1.

M^*	Case	D	k	a	RCCI	RCCD
	H1	$6.3 \cdot 10^3$	0.6985	$1/1.20$ days^{-1}	-0.005	-0.005
$\hat{M}_{\mathrm{H2}}$	H2	$6.5 \cdot 10^3$	0.6945	$1/4.27$ days^{-1}	-0.005	-0.005
	H3	$1.4 \cdot 10^9$	0.7226	$1/27.4$ days^{-1}	-0.003	-0.003
	H1	$6.0 \cdot 10^3$	0.7387	$1/1.25$ days^{-1}	-0.005	-0.005
$\hat{M}_{\mathrm{nv}}$	H2	$6.5 \cdot 10^3$	0.6945	$1/4.27$ days^{-1}	-0.005	-0.005
	H3	$4.7 \cdot 10^8$	0.9960	$1/5.89$ days^{-1}	-0.006	-0.005

of D, k, and a are reported in Table 2 for both the cases $M^* = \hat{M}_{\mathrm{H2}}$ and $M^* = \hat{M}_{\mathrm{nv}}$. From Table 2, we note that D_{H1} and D_{H2} are of the same order of magnitude (indeed, $D_{\mathrm{H2}}M^* \ll 1$ in (4.4)), while D_{H3} is about five orders of magnitude greater than D_{H2}. As for the information coverage k, we note that when $M^* = \hat{M}_{\mathrm{H2}}$, we get similar values independently of the considered Holling functions. On the other hand, when $M^* = \hat{M}_{\mathrm{nv}}$, the information coverage "jumps" to $k = 0.9960 \approx 1$ in case H3. Finally, we note that the average information delay, $1/a$, is almost always less than a week, except for case H3 and $M^* = \hat{M}_{\mathrm{H2}}$, where $1/a = 27.4$ days.

An immediate consequence of the parametrisation above is that information-related parameter values have almost no relevant changes when the Holling type II vaccination rate is replaced by the Holling type I vaccination rate. On the contrary, comparing the official data of 2016/2017 Nigerian outbreak with the solutions of SCVIR–M model under the assumption of Holling type III vaccination rate leads to higher and possibly unrealistic values of D, k, and $1/a$. Indeed, we get $k \approx 1$ when $M^* = \hat{M}_{\mathrm{nv}}$, which leads to the unlikely circumstance of no under-reporting [35]. We also obtain $1/a = 27.4$ days, when $M^* = \hat{M}_{\mathrm{H2}}$, which indicates that the information took an extremely long time to reach the public. This suggests that the Holling type III vaccination rate is the least suitable formulation to represent the vaccination rate in this field case.

5. Testing Holling functionals via SCVIR–M model

In this section, we test the capability of reproducing real data of the SCVIR–M model where the population's response to the information is represented, in turn, by the different Holling functionals. We begin by using the SCVIR–M model to reproduce the suspected cases and deaths caused by the 2016/2017 meningitis outbreak in Nigeria. The available data refer to weekly reports produced by the Nigeria Centre for Disease Control starting from the epidemiological week 50 of year 2016 [29]. Since a suspected case of meningitis is defined as a person with high fever and at least one of the meningeal signs [36], we do not distinguish between suspected cases and confirmed cases of illness (therefore,

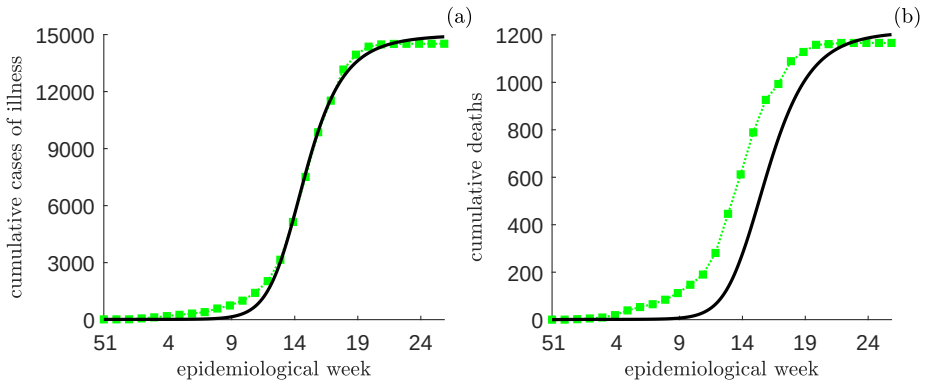

Figure 2. Comparison between the official data of 2016/2017 Nigerian meningitis outbreak (square markers) and the solutions of SCVIR–M model with Holling type II vaccination rate (solid lines). Panel (a): cumulative cases of illness. Panel (b): cumulative deaths. The ticks on the horizontal axis correspond to the first day of the indicated epidemiological week, starting from the week 51 of year 2016 until the week 25 of year 2017. Initial conditions and parameter values are given in Tables 1 and 2.

the suspected cases are described by the variable I in the model (2.1)). Using the parameter values in Tables 1 and 2, the SCVIR–M model satisfactorily reproduces the cumulative curves of cases of illness and deaths (see Figure 2), although the latter shows a delay possibly due to the procedure used to collect the data. Indeed, the deceased individuals have been probably recorded at the time of onset of the disease and not at the time of their death [17].

The solutions shown in Figure 2 refer to the SCVIR–M model with Holling type II vaccination rate. To emphasise the differences among the cases H1, H2, and H3, we introduce the index

$$\mathrm{RC}X = \frac{X - X^0}{X^0}, \tag{5.1}$$

which measures the percentage relative change of the quantity X w.r.t. the corresponding value X^0 as predicted in the *unresponsive* case. The unresponsive case occurs when circulating information and rumours on the status of the disease do not affect the vaccination behaviour (that is, X^0 is the value of X as predicted by the SCVIR–M model with $p_1(M) = 0$).

Given the time interval $\mathcal{I} = [0, t_f]$, we take $X \in \{\mathrm{CI}, \mathrm{CD}\}$, where CI and CD are the total number of cases of illness and deaths, respectively, in $\mathcal{I}$. We have:

$$\mathrm{CI} = \int_0^{t_f} \sigma C(t)dt, \quad \mathrm{CD} = \int_0^{t_f} \nu I(t)dt. \tag{5.2}$$

The obtained results are reported in the last two columns of Table 2. We note that in cases H1 and H2, the information-dependent vaccination rate produces a decrease of about 0.5% of both the quantities CI and CD w.r.t. the unresponsive case. Similar results hold in case H3 when $M^* = \hat{M}_{\mathrm{nv}}$. At variance, in case H3 when $M^* = \hat{M}_{\mathrm{H2}}$, we observe a smaller impact of human behaviour on quantities (5.2) since the value of both RCCI and RCCD is about 0.3%. This last result could be related to the very high average information delay estimated in such a case ($1/a = 27.4$ days). Note that, as can be inferred from the minimal differences in the values of RCCI (resp. RCCD) among the cases H1, H2, and H3,

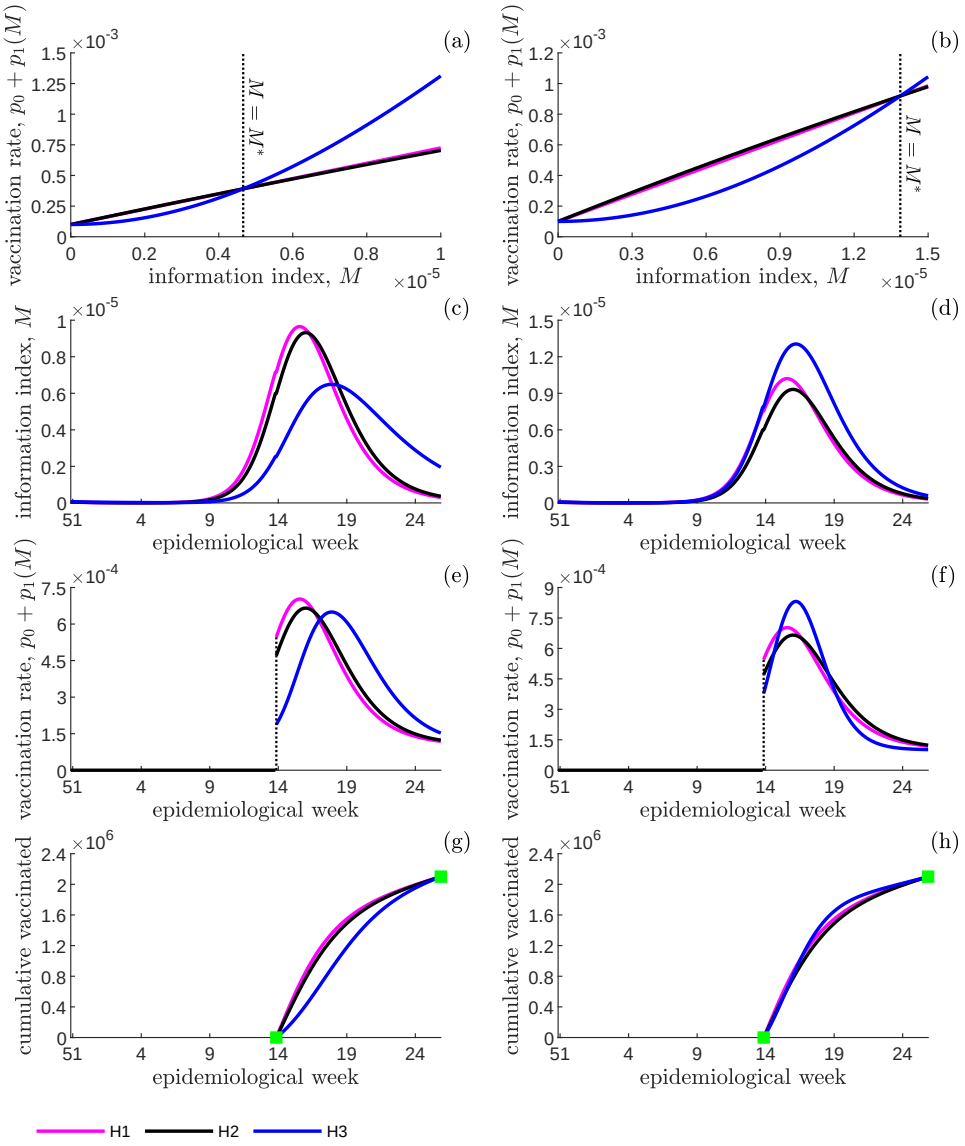

Figure 3. Panels (a)–(c)–(e)–(g): case $M^* = \hat{M}_{\mathrm{H2}}$. Panels (b)–(d)–(f)–(h): case $M^* = \hat{M}_{\mathrm{nv}}$. Panels (a)–(b): vaccination rate $p_0 + p_1(M)$ as a function of M. Panels (c)–(d): temporal dynamics of the information index M. Panels (e)–(f): temporal dynamics of the vaccination rate $p_0 + p_1(M)$. Panel (g)–(h): temporal dynamics of the cumulative number of vaccinated individuals. H1 lines: simulations by SCVIR–M model with Holling type I vaccination rate. H2 lines: simulations by SCVIR–M model with Holling type II vaccination rate. H3 lines: simulations by SCVIR–M model with Holling type III vaccination rate. The square markers indicate the official number of vaccinated individuals during the 2016/2017 meningitis outbreak in Nigeria [29]. The ticks on the horizontal axis correspond to the first day of the indicated epidemiological week, starting from the week 51 of year 2016 until the week 25 of year 2017. Initial conditions and parameter values are given in Tables 1 and 2.

the trends of cumulative cases of illness (resp. cumulative deaths) are nearly identical. For this reason, in Figure 2 we do not present the plots for cases H1 and H3 that visually overlap with those shown for

case H2.

We now compare the vaccination-related quantities (i.e., vaccination rate, information index, and cumulative vaccinated individuals) as predicted by the SCVIR–M model in cases H1, H2, H3. We note that cases H1 and H2 produce similar vaccination dynamics (see Figure 3). Indeed, in our parameter settings, the Holling type II vaccination rate behaves like a linear function of M (see Figures 3a and 3b). At variance, in case H3 and $M^* = \hat{M}_{\mathrm{H2}}$, we note that the peak reached by the information index M during the outbreak is delayed and lower w.r.t. cases H1 and H2 (Figure 3c), with a consequent delay in the peak of the vaccination rate (see Figure 3e). As a consequence, comparing H3 to cases H1 and H2, the cumulative number of vaccinated individuals increases slower in the initial phase of the vaccination campaign and faster during its final phase (see Figure 3g). Such differences are less relevant when $M^* = \hat{M}_{\mathrm{nv}}$ since the peak reached by both the information index and vaccination rate occurs almost at the same time for all Holling cases (see Figures 3d and 3f). In this scenario, the cumulative vaccinated curves are similar (see Figure 3h).

6. Conclusions

In this paper, we focus on the formulation of the functions that describe the population's response to the information during an epidemic. In particular, we test the performance of the Holling functional responses by using a socio-epidemiological model describing the spread of meningococcal meningitis. The main aim is to select the Holling functional response that best represents vaccination behaviour during a meningitis outbreak for which official data are available.

Our analysis, using data on cases of illness and deaths during the 2016/2017 meningitis outbreak in Nigeria, shows that any of the Holling vaccination rates allows to properly reproduce the data. However, the time evolution of the state variables for which data are not available (e.g., vaccinated individuals) may differ significantly when the Holling type III functional is used as vaccination rate. Moreover, in this case, the values of the information parameters appear to be out of scale compared to what could be expected in real cases (for example, we obtain an overestimated characteristic memory time). Therefore, the Holling type I and type II functionals appear to be more suitable than type III in representing the vaccination behaviour of the population.

In many theoretical and applied investigations where behavioural models are used to describe epidemic outbreaks, the Holling type II functional is typically used to describe the human response to information [14, 16, 17]. Here, we show that employing the Holling type II as vaccination rate allows both to properly reproduce the official data and to obtain reasonable estimates of the information parameters. A vaccination rate depending linearly on the information index might be a valid alternative. However, this requires a discontinuity jump of $p_1'(M)$, i.e., the speed of the population response to information changes, and currently there are no enough data available to justify such a discontinuity. Another shortcoming of using a Holling type I functional is that the characteristic memory time appears to be underestimated (the information would only need around 30 hours to reach the general public).

The above considerations confirm the adequacy of choosing the Holling type II functional response as vaccination rate. Given the interpretation of this functional in the context of socio-epidemiology (see Section 3), this means that susceptible individuals need time to handle the available information and that the *speed* at which they come into contact with information may be assumed to be constant.

Our work presents some limitations. First of all, although we provide a bifurcation analysis showing

that endemic states are possible for $\mathcal{R}_V > 1$, a complete analysis of the endemic equilibria, including their number and stability, is still open. When the function $p_1(\cdot)$ is assigned, the number of endemic equilibria may be obtained through the equation (A.6). An example is given in [17], where it is proven that the SCVIR–M model admits either zero or two endemic equilibria if $\mathcal{R}_V < 1$, and it admits either one or three endemic equilibria if $\mathcal{R}_V > 1$.

Another important issue concerns the estimates of the information parameters. We point out that in our study, they are estimated by using vaccination data and a specific metric (Equation (4.5)). Such estimates could be, in principle, directly obtained through surveys assessing the vaccination attitudes of individuals as well as their risk perception of disease and vaccination. For example, the result of the survey [33] regarding meningitis risk in Northern Ghana revealed that 100% of people surveyed identified meningitis as a serious disease and, even if more than 64% of them had been vaccinated, only 33% believed the vaccine was truly effective. This circumstance seems to indicate a vaccination behaviour induced by the fear of the disease, which could be modelled as a high value of the parameter k in (2.4). While some surveys are available in literature [33, 37–39], there is still a lack of studies where attitudes and risk perception regarding meningitis vaccination are directly linked to information and rumours.

While the interpretation provided in Section 3 is a first step to identify the correct formulation of the population's response to information, a fundamental factor remains how to estimate the parameters. Here, we use a parameter setting obtained through a comparison of model solutions with official data [17]. It would be valuable to confirm our results by using parameter estimation obtained through appropriate MCMC methods [40]. This will be the subject of future investigations.

Use of AI tools declaration

The authors declare they have not used Artificial Intelligence (AI) tools in the creation of this article.

Acknowledgments

We sincerely thank the editor and reviewers for their careful reading and insightful comments, which have greatly helped improve our manuscript. This work has been performed under the auspices of the Italian National Group for Mathematical Physics (GNFM) of the National Institute for Advanced Mathematics (INdAM).

This research was supported by EU funding within the NextGenerationEU—MUR PNRR Extended Partnership initiative on Emerging Infectious Diseases (Project no. PE00000007, INF-ACT).

B.B. also acknowledges PRIN 2020 project (No. 2020JLWP23) "Integrated Mathematical Approaches to Socio–Epidemiological Dynamics".

Conflict of interest

The authors declare there is no conflict of interest.

A. Qualitative analysis

Let us begin by looking for equilibria of the SCVIR–M model such that $C = I = 0$. The only *disease–free equilibrium* (DFE) is given by

$$\text{DFE} = \left(\bar{S}, \bar{V}, 0, 0, 0, 0\right) = \left(\frac{\Lambda(\theta+\mu)}{\mu(p_0+\theta+\mu)}, \frac{\Lambda p_0}{\mu(p_0+\theta+\mu)}, 0, 0, 0, 0\right). \tag{A.1}$$

Note that $\bar{S} + \bar{V} = \bar{N}$.

Proposition 1. *If $\mathcal{R}_V < 1$, where $\mathcal{R}_V$ is given in (2.9), then the DFE is locally asymptotically stable. If $\mathcal{R}_V > 1$, then the DFE is unstable.*

Proof. This result is a direct consequence of the next-generation matrix method used to obtain $\mathcal{R}_V$ (see [41]).

Proposition 2. *If $\mathcal{R}_0 \leq 1$, where $\mathcal{R}_0$ is given in (2.8), then the DFE is globally asymptotically stable.*

Proof. We adopt the approach developed by Kamgang and Sallet [42]. System (2.1) may be rewritten in the form

$$\begin{aligned} \dot{x}_1 &= A_1(x)(x_1 - x_1^0) + A_{12}(x)x_2 \\ \dot{x}_2 &= A_2(x)x_2, \end{aligned} \tag{A.2}$$

where $x = (x_1, x_2)$, being $x_1 = (S, V, R, M)^T$ and $x_2 = (C, I)^T$ the vectors of uninfected and infected compartments, respectively. Using such notations, the DFE may be written $(x_1^0, 0, 0)^T$, where $x_1^0 = (\bar{S}, \bar{V}, 0, 0)$. One can easily verify that

$$A_1 = \begin{pmatrix} -(p_0+\mu) & \theta & \phi & -\dfrac{p_1(M)}{M}S \\ p_0 & -(\theta+\mu) & 0 & \dfrac{p_1(M)}{M}S \\ 0 & 0 & -(\phi+\mu) & 0 \\ 0 & 0 & 0 & -a \end{pmatrix},$$

$$A_{12} = \begin{pmatrix} -\dfrac{\beta}{N}S & -\dfrac{\beta}{N}S \\ -(1-\psi)\dfrac{\beta}{N}V & -(1-\psi)\dfrac{\beta}{N}V \\ \delta & \rho \\ 0 & ah \end{pmatrix},$$

and

$$A_2 = \begin{pmatrix} \dfrac{\beta}{N}(S + (1-\psi)V) - (\sigma+\delta+\mu) & \dfrac{\beta}{N}(S + (1-\psi)V) \\ \sigma & -(\rho+\mu+\nu) \end{pmatrix}. \tag{A.3}$$

Then, the DFE is globally asymptotically stable, provided that the following conditions are satisfied (see [42], Theorem 4.3):

C1. The system (A.2) is defined on a positively invariant region Ω of the nonnegative orthant, and is dissipative on Ω.

C2. The equilibrium x_1^0 is globally asymptotically stable for the sub-system $\dot{x}_1 = A_1(x_1, 0)(x_1 - x_1^0)$.
C3. The matrix A_2 is Metzler (i.e., the off-diagonal components are nonnegative) and irreducible.
C4. There exists an upper bound matrix $\tilde{A}_2$ for $\mathcal{M} = \{A_2(x),\ x \in \Omega\}$ with the property that either $\tilde{A}_2 \notin \mathcal{M}$ or if $\tilde{A}_2 \in \mathcal{M}$ (i.e., $\tilde{A}_2 = \max_\Omega \mathcal{M}$), then for any $\tilde{x} = (\tilde{x}_1, \tilde{x}_2) \in \Omega$ such that $\tilde{A}_2 = A_2(\tilde{x})$, it follows that $\tilde{x}_2 = 0$ (i.e., the points where the maximum is realised are contained in the disease-free sub-manifold).
C5. The stability modulus (i.e., the greatest real part of the eigenvalues) of $\tilde{A}_2$ is nonpositive.

Condition C1 is a direct consequence of (2.7). Condition C3 follows from (A.3). The sub-system mentioned in Condition C2 is

$$\begin{aligned}
\dot{S} &= \Lambda - (p_0 + p_1(M))\, S + \theta V + \phi R - \mu S \\
\dot{V} &= (p_0 + p_1(M))\, S - (\theta + \mu) V \\
\dot{R} &= -(\phi + \mu) R \\
\dot{M} &= -aM,
\end{aligned}$$

so that

$$(S, V, R, M) \to \left(\frac{\Lambda(\theta + \mu)}{\mu(p_0 + \theta + \mu)}, \frac{\Lambda p_0}{\mu(p_0 + \theta + \mu)}, 0, 0 \right), \text{ as } t \to +\infty.$$

Therefore, Condition C2 is also verified.

The matrix $\tilde{A}_2$ required by Conditions C4 and C5 is

$$\tilde{A}_2 = \begin{pmatrix} \beta - (\sigma + \delta + \mu) & \beta \\ \sigma & -(\rho + \mu + \nu) \end{pmatrix},$$

since $S + (1 - \psi)V \le S + V \le N$ in Ω, and $\tilde{A}_2 \in \mathcal{M}$ only if $S = N$ and $V = C = I = R = 0$, so that $\tilde{x}_2 = 0$ and the Condition C4 is fulfilled.

Finally, all the eigenvalues of $\tilde{A}_2$ have a nonpositive real part if, and only if, $\det(\tilde{A}_2) \ge 0$ and $\mathrm{tr}(\tilde{A}_2) \le 0$, which is equivalent to

$$\beta\,(\rho + \mu + \nu + \sigma) \le (\sigma + \delta + \mu)(\rho + \mu + \nu),$$

i.e., to the hypothesis $\mathcal{R}_0 \le 1$. Therefore, Condition C5 is also satisfied. □

Now, we investigate the existence of *endemic* equilibria (EE) of the SCVIR–M model, i.e., equilibria such that $C \neq 0$ and $I \neq 0$. Let us denote by $\mathrm{EE} = (S_e, V_e, C_e, I_e, R_e, M_e)$ the generic endemic equilibrium and, for convenience, introduce the quantities:

$$q_1 = \theta + \mu, \quad q_2 = \sigma + \delta + \mu, \quad q_3 = \rho + \mu + \nu, \quad q_4 = \phi + \mu. \tag{A.4}$$

From the SCVIR–M model, the components of EE can be written as functions of $\lambda_e = \beta(C_e + I_e)/N_e$, where N_e is the size of the total population at the endemic equilibrium, i.e., $N_e = (\Lambda - \nu I_e)/\mu$. One

gets:

$$\begin{aligned} S_e &= \frac{(1-\psi)\lambda_e + q_1}{(1-\psi)(\lambda_e + p_e) + q_1} \frac{\Lambda q_2 q_3}{\beta\mu(q_3+\sigma) + \sigma\nu\lambda_e} \\ V_e &= \frac{p_e}{(1-\psi)(\lambda_e + p_e) + q_1} \frac{\Lambda q_2 q_3}{\beta\mu(q_3+\sigma) + \sigma\nu\lambda_e} \\ C_e &= \frac{\Lambda q_3 \lambda_e}{\beta\mu(q_3+\sigma) + \sigma\nu\lambda_e} \\ I_e &= \frac{\Lambda\sigma\lambda_e}{\beta\mu(q_3+\sigma) + \sigma\nu\lambda_e} \\ R_e &= \frac{\Lambda(\delta q_3 + \sigma\rho)\lambda_e}{q_4(\beta\mu(q_3+\sigma) + \sigma\nu\lambda_e)} \\ M_e &= \frac{h\Lambda\sigma\lambda_e}{\beta\mu(q_3+\sigma) + \sigma\nu\lambda_e}, \end{aligned} \tag{A.5}$$

where $p_e = p_0 + p_1(M_e)$.

Then, once a specific functional shape is attributed to $p_1(\cdot)$, one can obtain the possible values of λ_e as the positive roots of the r.h.s. of the first equation in (2.1), namely:

$$\Lambda - (\lambda_e + p_e + \mu)\, S_e + \theta V_e + \phi R_e = 0, \tag{A.6}$$

where S_e, V_e and R_e are given in (A.5).

Proposition 3. *The SCVIR–M model exhibits a forward (resp. backward) bifurcation at DFE and* $\mathcal{R}_V = 1$ *if*

$$\psi(w_1\bar{V} - w_2\bar{S}) - (w_3 + w_4 + w_5)(\bar{S} + (1-\psi)\bar{V}) < 0 \quad (resp. > 0),$$

where $\bar{S}$, $\bar{V}$ *are given in (A.1) and*

$$\begin{aligned} w_1 &= \left(\frac{\phi(\delta q_3 + \sigma\rho) - q_2 q_3 q_4}{\sigma q_4 \mu}\right) w_4 - w_2 \\ w_2 &= \frac{w_4}{\sigma(p_0 + q_1)} \left(p_0 \frac{\phi(\delta q_3 + \sigma\rho) - q_2 q_3 q_4}{q_4 \mu} + \beta_c \frac{\bar{S}}{\bar{N}} (q_3 + \sigma) - q_2 q_3 + p_1'(0) h\sigma\bar{S}\right) \\ w_3 &= \frac{q_3}{\sigma} w_4 \\ w_4 &= \frac{q_2\sigma}{q_3(q_3+\sigma) + q_2\sigma} \\ w_5 &= \frac{\delta q_3 + \sigma\rho}{\sigma q_4} w_4. \end{aligned}$$

Proof. See paper [17].

In case of backward bifurcation, when $\mathcal{R}_V < 1$, with $|\mathcal{R}_V - 1| \ll 1$, the DFE is locally asymptotically stable, and there exists an unstable endemic equilibrium; when $\mathcal{R}_V > 1$, with $\mathcal{R}_V - 1 \ll 1$, the DFE is unstable. At variance, in case of forward bifurcation, when $\mathcal{R}_V - 1$ changes from negative to positive, the locally asymptotically stable DFE becomes unstable, and a locally asymptotically stable endemic equilibrium emerges.

References

1. J. Bedford, J. Farrar, C. Ihekweazu, G. Kang, M. Koopmans, J. Nkengasong, A new twenty-first century science for effective epidemic response, *Nature*, **575** (2019), 130–136. https://doi.org/10.1038/s41586-019-1717-y
2. D. Weston, A. Ip, R. Amlôt, Examining the application of behaviour change theories in the context of infectious disease outbreaks and emergency response: A review of reviews, *BMC Public Health*, **20** (2020), 1483. https://doi.org/10.1186/s12889-020-09519-2
3. S. Funk, M. Salathé, V. A. Jansen, Modelling the influence of human behaviour on the spread of infectious diseases: a review, *J. R. Soc. Interface*, **7** (2010), 1247–1256. http://doi.org/10.1098/rsif.2010.0142
4. P. Manfredi, A. d'Onofrio, *Modeling the Interplay Between Human Behavior and the Spread of Infectious Diseases*, Springer, New York, 2013. https://doi.org/10.1007/978-1-4614-5474-8
5. Z. Wang, C. T. Bauch, S. Bhattacharyya, A. d'Onofrio, P. Manfredi, M. Perc, et al., Statistical physics of vaccination, *Phys. Rep.*, **664** (2016), 1–113. https://doi.org/10.1016/j.physrep.2016.10.006
6. V. Capasso, *Mathematical Structures of Epidemic Systems*, Springer, Berlin, 1993. https://doi.org/10.1007/978-3-540-70514-7
7. V. Capasso, G. Serio, A generalization of the Kermack–McKendrick deterministic epidemic model, *Math. Biosci.*, **42** (1978), 43–61. https://doi.org/10.1016/0025-5564(78)90006-8
8. S. Funk, E. Gilad, C. Watkins, V. A. A. Jansen, The spread of awareness and its impact on epidemic outbreaks, *PNAS*, **106** (2009), 6872–6877. https://doi.org/10.1073/pnas.0810762106
9. M. Riera-Montes, I. Velicko, The Chlamydia surveillance system in Sweden delivers relevant and accurate data: results from the system evaluation, 1997–2008, *Euro Surveill.*, **16** (2011), 19907. https://doi.org/10.2807/ese.16.27.19907-en
10. A. d'Onofrio, P. Manfredi, Bistable endemic states in a susceptible–infectious–susceptible model with behavior–dependent vaccination, in *Mathematical and Statistical Modeling for Emerging and Re–emerging Infectious Diseases* (eds. G. Chowell and J. M. Hyman), Springer, Cham, 2016, 341–354. https://doi.org/10.1007/978-3-319-40413-4_21
11. B. Buonomo, A. d'Onofrio, D. Lacitignola, Global stability of an SIR epidemic model with information dependent vaccination, *Math. Biosci.*, **216** (2008), 9–16. https://doi.org/10.1016/j.mbs.2008.07.011
12. A. d'Onofrio, P. Manfredi, Information–related changes in contact patterns may trigger oscillations in the endemic prevalence of infectious diseases, *J. Theor. Biol.*, **256** (2009), 473–478. https://doi.org/10.1016/j.jtbi.2008.10.005
13. A. d'Onofrio, P. Manfredi, E. Salinelli, Vaccinating behaviour, information, and the dynamics of SIR vaccine preventable diseases, *Theor. Popul. Biol.*, **71** (2007), 301–317. https://doi.org/10.1016/j.tpb.2007.01.001
14. B. Buonomo, R. Della Marca, A. d'Onofrio, M. Groppi, A behavioural modelling approach to assess the impact of COVID–19 vaccine hesitancy, *J. Theor. Biol.*, **534** (2022), 110973. https://doi.org/10.1016/j.jtbi.2021.110973

15. C. Zuo, Y. Ling, F. Zhu, X. Ma, G. Xiang, Exploring epidemic voluntary vaccinating behavior based on information-driven decisions and benefit-cost analysis, *Appl. Math. Comput.*, **447** (2023), 127905. https://doi.org/10.1016/j.amc.2023.127905

16. B. Buonomo, R. Della Marca, Effects of information–induced behavioural changes during the COVID–19 lockdowns: the case of Italy, *R. Soc. Open Sci.*, **7** (2020), 201635. https://doi.org/10.1098/rsos.201635

17. B. Buonomo, R. Della Marca, A behavioural vaccination model with application to meningitis spread in Nigeria, *Appl. Math. Model.*, **125** (2024), 334–350. https://doi.org/10.1016/j.apm.2023.09.031

18. O. Andersson, P. Campos-Mercade, A. N. Meier, E. Wengström, Anticipation of COVID–19 vaccines reduces willingness to socially distance, *J. Health Econ.*, **80** (2021), 102530. https://doi.org/10.1016/j.jhealeco.2021.102530

19. B. Buonomo, R. Della Marca, S. S. Sharbayta, A behavioral change model to assess vaccination-induced relaxation of social distancing during an epidemic, *J. Biol. Syst.*, **30** (2022), 1–25. https://doi.org/10.1142/S0218339022500085

20. A. Kumar, P. K. Srivastava, Y. Dong, Y. Takeuchi, Optimal control of infectious disease: Information–induced vaccination and limited treatment, *Phys. A*, **542** (2020), 123196. https://doi.org/10.1016/j.physa.2019.123196

21. C. S. Holling, The components of predation as revealed by a study of small-mammal predation of the European pine sawfly, *Can. Entomol.*, **91** (1959), 293–320. http://doi.org/10.4039/Ent91293-5

22. C. S. Holling, Some characteristics of simple types of predation and parasitism, *Can. Entomol.*, **91** (1959), 385–398. http://doi.org/10.4039/Ent91385-7

23. J. P. DeLong, *Predator Ecology: Evolutionary Ecology of the Functional Response*, Oxford University Press, Oxford, 2021, https://doi.org/10.1093/oso/9780192895509.001.0001

24. F. Agusto, M. Leite, Optimal control and cost–effective analysis of the 2017 meningitis outbreak in Nigeria, *Infect. Dis. Model.*, **4** (2019), 161–187. https://doi.org/10.1016/j.idm.2019.05.003

25. G. Djatcha Yaleu, S. Bowong, E. H. Danga, J. Kurths, Mathematical analysis of the dynamical transmission of Neisseria meningitidis serogroup A, *Int. J. Comput. Math.*, **94** (2017), 2409–2434. https://doi.org/10.1080/00207160.2017.1283411

26. Centers for Disease Control and Prevention, Meningococcal Disease, Available from: `https://www.cdc.gov/meningococcal/index.html`, 2023, (Accessed on September 2024).

27. World Health Organization, Meningitis, Available from: `https://www.who.int/news-room/fact-sheets/detail/meningitis`, 2023, (Accessed on October 2024).

28. N. MacDonald, *Biological Delay Systems: Linear Stability Theory*, Cambridge University Press, Cambridge, 1989.

29. Nigeria Centre for Disease Control and Prevention, An update of meningitis outbreak in Nigeria, Available from: `https://www.ncdc.gov.ng/ncdc.gov.ng/diseases/sitreps/?cat=6&name=An%20Update%20of%20Meningitis%20Outbreak%20in%20Nigeria`, 2022, (Accessed on November 2024).

30. C. Nnadi, J. Oladejo, S. Yennan, A. Ogunleye, C. Agbai, L. Bakare, et al., Large outbreak of Neisseria meningitidis Serogroup C – Nigeria, December 2016–June 2017, *Morb. Mortal. Wkly Rep.*, **66** (2017), 1352–1356. https://doi.org/10.15585/mmwr.mm6649a3

31. World Health Organization Africa, End of meningitis outbreak in Nigeria, December 2016–June 2017, Available from: https://www.afro.who.int/sites/default/files/2017-09/Dashboard%20of%20Nigeria%20meningitis%20-%20EndF.pdf, 2017, (Accessed on November 2024).

32. R. Falcone, A. Sapienza, Information seeking behavior at the time of COVID-19, in *Proceedings of the 22nd Workshop "From Objects to Agents"*, 2021, 241–258.

33. M. H. Hayden, M. Dalaba, T. Awine, P. Akweongo, G. Nyaaba, D. Anaseba, et al., Knowledge, attitudes, and practices related to meningitis in northern Ghana, *Am. J. Trop. Med. Hyg.*, **89** (2013), 265–270. https://doi.org/10.4269/ajtmh.12-0515

34. MATLAB, Matlab release 2023a. The MathWorks, Inc., Natick, MA, 2023.

35. C. Azzari, F. Nieddu, M. Moriondo, G. Indolfi, C. Canessa, S. Ricci, et al., Underestimation of invasive meningococcal disease in Italy, *Emerg. Infect. Dis.*, **22** (2016), 469–475. https://doi.org/10.3201/eid2203.150928

36. World Health Organization, Meningitis outbreak response in sub–Saharan Africa, Available from: https://www.who.int/publications/i/item/WHO-HSE-PED-CED-14.5, 2014, (Accessed on July 2024).

37. I. Ballalai, R. Dawson, M. Horn, V. Smith, R. Bekkat-Berkani, L. Soumahoro, et al., Understanding barriers to vaccination against invasive meningococcal disease: A survey of the knowledge gap and potential solutions, *Expert Rev. Vaccines*, **22** (2023), 457–467. https://doi.org/10.1080/14760584.2023.2211163

38. B. Murele, R. Vaz, A. Gasasira, P. Mkanda, T. Erbeto, J. Okeibunor, Vaccine perception among acceptors and non-acceptors in Sokoto State, Nigeria, *Vaccine*, **32** (2014), 3323–3327. https://doi.org/10.1016/j.vaccine.2014.03.050

39. D. R. Timmermans, L. Henneman, R. A. Hirasing, G. Van der Wal, Attitudes and risk perception of parents of different ethnic backgrounds regarding meningococcal C vaccination, *Vaccine*, **23** (2005), 3329–3335. https://doi.org/10.1016/j.vaccine.2005.01.075

40. G. I. Valderrama-Bahamóndez, H. Fröhlich, MCMC techniques for parameter estimation of ODE based models in systems biology, *Front. Appl. Math. Stat.*, **5** (2019). https://doi.org/10.3389/fams.2019.00055

41. P. Van den Driessche, J. Watmough, Reproduction numbers and sub–threshold endemic equilibria for compartmental models of disease transmission, *Math. Biosci.*, **180** (2002), 29–48. https://doi.org/10.1016/S0025-5564(02)00108-6

42. J. C. Kamgang, G. Sallet, Computation of threshold conditions for epidemiological models and global stability of the disease-free equilibrium (DFE), *Math. Biosci.*, **213** (2008), 1–12. https://doi.org/10.1016/j.mbs.2008.02.005

AIMS Press